

# Linköping University Postprint

## Current statistics for wave transmission through an open Sinai billiard: Effects of net currents

Almas F. Sadreev and Karl-Fredrik Berggren

**N.B.:** When citing this work, cite the original article.

Original publication:

Almas F. Sadreev and Karl-Fredrik Berggren, Current statistics for wave transmission through an open Sinai billiard: Effects of net currents, 2004, Physical Review E, (70), 026201.

<http://dx.doi.org/10.1103/PhysRevE.70.026201>.

Copyright: The American Physical Society, <http://prb.aps.org/>

Postprint available free at:

Linköping University E-Press: <http://urn.kb.se/resolve?urn=urn:nbn:se:liu:diva-12554>

# Current statistics for wave transmission through an open Sinai billiard: Effects of net currents

Almas F. Sadreev<sup>1,2,3</sup> and Karl-Fredrik Berggren<sup>1</sup>

<sup>1</sup>*Department of Physics and Measurement Technology, Linköping University, S-581 83 Linköping, Sweden*

<sup>2</sup>*Kirensky Institute of Physics, 660036 Krasnoyarsk, Russia*

<sup>3</sup>*Astaf'ev Krasnoyarsk Pedagogical University, 660049 Lebedeva, Krasnoyarsk, Russia*

(Received 7 February 2004; published 9 August 2004)

Transport through quantum and microwave cavities is studied by analytic and numerical techniques. In particular, we consider the statistics for a finite net probability current (Poynting vector) ( $\mathbf{j}$ ) flowing through an open ballistic Sinai billiard to which two opposite leads/wave guides are attached. We show that if the net probability current is small, the scattering wave function inside the billiard is well approximated by a Gaussian random complex field. In this case, the current statistics are universal and obey simple analytic forms. For larger net currents, these forms still apply over several orders of magnitudes. However, small characteristic deviations appear in the tail regions. Although the focus is on electron and microwave billiards, the analysis is relevant also to other classical wave cavities as, for example, open planar acoustic reverberation rooms, elastic membranes, and water surface waves in irregularly shaped vessels.

DOI: 10.1103/PhysRevE.70.026201

PACS number(s): 05.45.Mt, 05.60.Gg, 73.23.Ad

## I. INTRODUCTION

Historically, McDonald and Kaufman revealed numerically the complicated morphology of the eigenstates in a closed two-dimensional Bunimovich billiard [1]. As is now well known, the statistics of major eigenfunction amplitudes follow a Gaussian distribution. The statistics of the squared amplitudes (the probability density for the case of quantum billiard) then obeys the Porter-Thomas distribution [2] as described by the Gaussian orthogonal ensemble (GOE). This kind of statistic has been observed experimentally for microwave cavities [3,4] and acoustic resonators [5,6]. These general observations do not apply to wave functions that are scarred along unstable periodic orbits, or show regular patterns associated with bouncing ball motion [7]. Such states are, however, more rare.

Here we consider what happens when a two-dimensional billiard is made open by attaching two wave guides (or leads) and a stationary transport through the system takes place. In the case of electrons, for example, a current may be induced by applying a small voltage between the two leads. The additional flexibility gained in this way gives rise to a number of interesting cases for the scattering wave-function statistics. By assuming that the scattering function forms a random Gaussian complex field, these cases were considered in [8–10]. In bypassing previous analytical results for wave-function statistics [11–14] were recovered also for this kind of open billiards [9,10].

Another rich system for studying “wave-function” properties and transport is a microwave resonator consisting of a planar waveguide, whose geometry is chosen to match that of some specific billiard system [3,14–17]. For TM modes the two-dimensional complex scattering function,

$$\psi(\mathbf{x}) = u(\mathbf{x}) + iv(\mathbf{x}), \quad (1)$$

obeys the Helmholtz equation,

$$(\nabla^2 + k^2)\psi = 0, \quad (2)$$

with the Dirichlet boundary conditions throughout. A schematic view of the system is shown in Fig. 1. The energy flow between input and output waveguides is given by the Poynting vector  $\mathbf{j} = \text{Im}(\psi^* \nabla \psi)$ . There is also a close similarity between electron transport and microwaves with acoustic waves [18]. Neumann boundary conditions are to be imposed in this case, but as before, there is an energy flow very much like the Poynting vector.

As indicated, there is thus a close formal similarity between (noninteracting) electron transport and microwave propagation in open quantum dots and microwave cavities, respectively. There is, however, a subtle difference. Electron transport is usually multichannel (channel refers to the transverse modes in the leads). The total current is therefore the sum of contributions from all states at the Fermi energy. Microwaves, the other hand, are injected as single-mode states. When comparing electron and microwave transport we should therefore restrict ourselves to monochromatic single-mode issues.

Based on an assumption that  $u$  and  $v$  in (1) are both random Gaussian fields, the probability current statistics were studied both analytically and numerically for transport

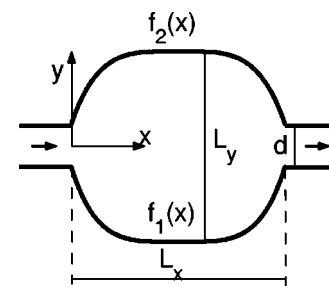


FIG. 1. Schematic geometry of an open hard-walled billiard with a net current in the  $x$  direction. Functions  $f_1(x)$  and  $f_2(x)$  define the boundaries of the cavity.

TABLE I. Numerically computed mean values.

Cases	$\omega^2$	$T$	$\epsilon$	$\langle p^2 \rangle$	$\langle q^2 \rangle$	$r$	$\frac{\langle p_x^2 \rangle}{k^2}$	$\frac{\langle q_x^2 \rangle}{k^2}$	$\frac{\langle pq_x \rangle}{k}$	$\frac{\langle qp_x \rangle}{k}$	$\frac{\langle p^2 \rangle \langle q_x^2 \rangle}{k^2}$	$\frac{\langle q^2 \rangle \langle p_x^2 \rangle}{k^2}$	$\frac{D_1}{k^2}$	$\frac{D_2}{k^2}$	$\frac{\langle j_x \rangle}{k}$	$\frac{\langle j \rangle}{k}$
A	12.1	0.002	67.37	$2.2 \times 10^{-4}$	0.9998	0.9996	0.513	$1.2 \times 10^{-4}$	$-1.3 \times 10^{-5}$	$1.74 \times 10^{-5}$	$1.18 \times 10^{-4}$	$1.13 \times 10^{-4}$	$1.19 \times 10^{-4}$	$1.13 \times 10^{-4}$	$3 \times 10^{-5}$	0.016
B	12.137	0.951	0.377	0.875	0.125	0.5625	0.504	0.046	0.012	-0.011	0.04	0.0628	0.04	0.0627	0.023	0.373
C	31.125	0.995	0.4209	0.85	0.15	0.490	0.384	0.109	0.031	-0.032	0.0925	0.058	0.0915	0.0568	0.063	0.391
D	31.20	0.549	0.2531	0.94	0.06	0.774	0.293	0.05	0.018	-0.018	0.046	0.0196	0.0456	0.0173	0.036	0.257

through a Bunimovich billiard [10]. Using the one-to-one correspondence between the Poynting vector in a microwave billiard and the probability current density, Barth and Stöckmann obtained a good agreement with theoretical predictions [15]. Recently, Brouwer [19] considered the joint distribution  $I(\mathbf{r})=A|\psi(\mathbf{r})|^2$  and the magnitude of the normalized current density  $J(\mathbf{r})=(A/k)|\text{Im } \psi^* \nabla \psi|$ , where  $A$  is the area of billiard. His considerations are based on Berry's ansatz for a chaotic wave function [20],

$$\psi(\mathbf{r}) = \sum_{\mathbf{k}} a(\mathbf{k})e^{i\mathbf{k}\cdot\mathbf{r}}, \quad (3)$$

where the wave vectors  $\mathbf{k}$  are distributed homogeneously on a circle with constant radius  $|\mathbf{k}|$  and the coefficients  $a(\mathbf{k})$  are the random complex coefficients.

The current and wave-function statistics in [9,10] have focused on the particular situation when the net probability flow through the cavity is relatively small because of the particular choice of perpendicular leads. In practice one may then disregard the net current flow in relation to all other local currents induced within the cavity. This is obviously the same as saying that the distribution for  $\mathbf{j}$  is in practice isotropic. This follows in particular from (3). The purpose of this work is to go beyond this simplification. We will therefore consider the general case of a net current flowing from the input to the output leads through a chaotic billiard, as shown in Fig. 1. As mentioned, we will focus on the case of monochromatic single-mode transmission. Because the straight leads are opposite each other the current becomes more directional. By solving the true scattering problem numerically we demonstrate that the assumption that the in-cavity scattering function is a random Gaussian field is quite a good one for small net currents. However, with increasing net currents this assumption gradually becomes invalid. The effect of net currents in the current statistics was considered by Ebeling reverberation rooms [21,22]. Here we thus extend his work to open quantum and microwave billiards.

## II. THE CURRENT STATISTICS FOR ANISOTROPIC RANDOM GAUSSIAN FIELDS

First, following [10] we perform a phase transformation,

$$\psi(\mathbf{x}) \rightarrow e^{i\alpha} \psi(\mathbf{x}) = p(\mathbf{x}) + iq(\mathbf{x}), \quad (4)$$

to new fields  $p(\mathbf{x})$  and  $q(\mathbf{x})$  with the condition that the statistical average  $\langle pq \rangle = 0$ . This step eliminates phase ambiguity and ensures that the Gaussian random fields  $p$  and  $q$  are statistically independent. The phase transformation (4) corresponds to diagonalization of the quadratic form in the expression for the joint probability density

$$f(u,v) = \frac{1}{2\pi\sqrt{\langle u^2 \rangle \langle v^2 \rangle - \langle uv \rangle^2}} \exp \left\{ -\frac{1}{2(\langle u^2 \rangle \langle v^2 \rangle - \langle uv \rangle^2)} \times [\langle u^2 \rangle v^2 + \langle v^2 \rangle u^2 - 2\langle uv \rangle uv] \right\},$$

which is now replaced by the product of two independent probability densities

$$f(p, q) = f(p)f(q),$$

$$f(p) = \frac{1}{\sqrt{2\pi\langle p^2 \rangle}} \exp\left(-\frac{p^2}{2\langle p^2 \rangle}\right),$$

$$f(q) = \frac{1}{\sqrt{2\pi\langle q^2 \rangle}} \exp\left(-\frac{q^2}{2\langle q^2 \rangle}\right).$$

This step is a matter of convenience, which simplifies the calculation of the wave function and current distribution.

However, we may not assume that the space derivatives of fields are statistically independent of the fields. In fact, it follows from the expression for the current density

$$\mathbf{j} = p \nabla q - q \nabla p \quad (5)$$

that

$$\langle p \nabla q \rangle \neq \mathbf{0}, \quad \langle q \nabla p \rangle \neq \mathbf{0}, \quad (6)$$

if the mean current  $\langle \mathbf{j} \rangle \neq \mathbf{0}$ . Here we use the following definition of an average,

$$\langle \dots \rangle = \frac{1}{A} \int_A d^2\mathbf{r} \dots, \quad (7)$$

where  $A$  is the area to be sampled. In this work we let  $A$  be the area of the billiard. The inequalities (6) tell that the fields are anisotropic. In terms of the Berry wave function (3) the anisotropy means that the wave vectors  $\mathbf{k}$  follow a nonuniform angular distribution over a circle. However, we may assume that

$$\langle p \rangle = 0, \langle q \rangle = 0, \quad \langle \nabla p \rangle = \mathbf{0}, \quad \langle \nabla q \rangle = \mathbf{0},$$

assumptions which are completely justified by our computer simulations (see Table I).

In order to find the distribution for one component of the current density, say  $j_x$ , we introduce the Gaussian probability density  $f(p, p_x, q, q_x)$  [21,22]. The function and its corresponding characteristic functions are completely determined by the covariance matrix of the field variables

$$\mathbf{M} = \begin{pmatrix} \langle p^2 \rangle & \langle pq_x \rangle & \langle pq \rangle & \langle pp_x \rangle \\ \langle pq_x \rangle & \langle q_x^2 \rangle & \langle qq_x \rangle & \langle p_x q_x \rangle \\ \langle pq \rangle & \langle qq_x \rangle & \langle q^2 \rangle & \langle qp_x \rangle \\ \langle pp_x \rangle & \langle p_x q_x \rangle & \langle qp_x \rangle & \langle p_x^2 \rangle \end{pmatrix} \approx \begin{pmatrix} \langle p^2 \rangle & \langle pq_x \rangle & 0 & 0 \\ \langle pq_x \rangle & \langle q_x^2 \rangle & 0 & 0 \\ 0 & 0 & \langle q^2 \rangle & \langle qp_x \rangle \\ 0 & 0 & \langle qp_x \rangle & \langle p_x^2 \rangle \end{pmatrix}. \quad (8)$$

The structure of the matrix is a consequence of the symmetry properties of the correlation functions [21]. It also agrees with our numerical simulations for the wave transmission through the Sinai billiard (see Table I below). As seen from the table, the average  $\langle p^2 \rangle$  does not equal  $\langle q^2 \rangle$ . This is also true for the related pair  $\langle p_x^2 \rangle$  and  $\langle q_x^2 \rangle$ . The equality  $\langle pq_x \rangle = -\langle qp_x \rangle$  is, however, satisfied with good accuracy.

Following [22] we have for the probability density

$$f(p, p_x, q, q_x) = f(p, q_x)f(q, p_x),$$

$$f(p, q_x) = \frac{1}{2\pi\sqrt{D_1}} \exp\left\{-\frac{1}{2D_1}[\langle q_x^2 \rangle p^2 + \langle p^2 \rangle q_x^2 - 2\langle pq_x \rangle pq_x]\right\},$$

$$f(q, p_x) = \frac{1}{2\pi\sqrt{D_2}} \exp\left\{-\frac{1}{2D_2}[\langle p_x^2 \rangle q^2 + \langle q^2 \rangle p_x^2 + 2\langle pq_x \rangle qp_x]\right\}, \quad (9)$$

where

$$D_1 D_2 = \det(\mathbf{M}), \quad D_1 = \langle q_x^2 \rangle \langle p^2 \rangle - \langle pq_x \rangle^2,$$

$$D_2 = \langle p_x^2 \rangle \langle q^2 \rangle - \langle qp_x \rangle^2. \quad (10)$$

Numerical values of  $D_1$  and  $D_2$  are also collected in Table I. The general form for the characteristic function of a four-dimensional Gaussian field  $\Theta(a) = \langle e^{iaj_x} \rangle$  is a product of two characteristic functions

$$\Theta(a) = \Theta_1(a)\Theta_2(a), \quad (11)$$

where

$$\Theta_1(a) = \int dp dq_x f(p, q_x) e^{iapq_x} = \sqrt{\frac{D_1}{\langle p^2 \rangle \langle q_x^2 \rangle - (\langle pq_x \rangle - iaD_1)^2}},$$

$$\Theta_2(a) = \int dq dp_x f(q, p_x) e^{-iaqp_x} = \sqrt{\frac{D_2}{\langle q^2 \rangle \langle p_x^2 \rangle - (\langle qp_x \rangle + iaD_2)^2}}. \quad (12)$$

For the particular case  $\langle p^2 \rangle = \langle q^2 \rangle$ ,  $\langle p_x^2 \rangle = \langle q_x^2 \rangle$ , Ebeling [22] has derived the following distribution for the current component:

$$P(j_x) = \frac{1}{2\tau} \exp\left\{-\frac{|j_x|}{\tau} + \frac{\langle j_x \rangle j_x}{2\tau^2}\right\}, \quad (13)$$

where we introduced a parameter,

$$\tau^2 = \sqrt{D_1 D_2}, \quad (14)$$

which for the present case equals

$$\tau^2 = \langle p^2 \rangle \langle q_x^2 \rangle = \langle q^2 \rangle \langle p_x^2 \rangle = \frac{1}{2} k^2 \langle p^2 \rangle \langle q^2 \rangle.$$

As to be expected the net current gives rise to an asymmetric distribution  $P(j_x)$ . In the case that the net flow through the cavity is only a small fraction of the total induced flow we may, to a good approximation, drop the second term in the exponential factor. The symmetric form from [10],

$$P(j_x) = \frac{1}{2\tau} \exp\left(-\frac{|j_x|}{\tau}\right), \quad (15)$$

is then obtained.

Let us now consider the general case with  $\langle p^2 \rangle \neq \langle q^2 \rangle$  and  $\langle p_x^2 \rangle \neq \langle q_x^2 \rangle$ . The distribution  $P(j_x)$  may then be generated from  $\Theta(a)$  by the following integration:

$$P(j_x) = \left\langle \delta \left( j_x - p \frac{\partial q}{\partial x} + q \frac{\partial p}{\partial x} \right) \right\rangle = \frac{1}{2\pi} \int_{-\infty}^{\infty} \Theta(a) e^{iaj_x} da. \quad (16)$$

With the notations

$$\alpha_1 = \frac{\langle pq_x \rangle}{D_1}, \quad \alpha_2 = \frac{\langle qp_x \rangle}{D_2}, \quad \beta_1 = \frac{\langle p^2 \rangle \langle q_x^2 \rangle}{D_1^2}, \quad \beta_2 = \frac{\langle q^2 \rangle \langle p_x^2 \rangle}{D_2^2}, \quad (17)$$

we therefore obtain

$$P(j_x) = \frac{1}{2\pi\sqrt{D_1 D_2}} \int_{-\infty}^{\infty} \frac{e^{izj_x} dz}{\sqrt{(iz - \alpha_1)^2 - \beta_1} \sqrt{(iz + \alpha_2)^2 - \beta_2}}. \quad (18)$$

Numerical values of the averages in (17) are collected in Table I. With the special choice  $\alpha_1 = -\alpha_2$  and  $\beta_1 = \beta_2$  we recover expression (13).

### III. RELATION BETWEEN MEAN NET PROBABILITY CURRENT DENSITY AND TOTAL CURRENT

In order to estimate a mean value of the net probability current we consider transmission through a billiard of arbitrary form with two straight leads attached to the billiard in the  $x$  direction as in Fig. 1. For convenience we choose the single incident wave,

$$\psi_{\text{inc}}(x, y) = \frac{1}{\sqrt{k}} e^{ikx} \phi_n(y), \quad (19)$$

where  $k$  is the wave number, and the normalized function  $\phi_n(y)$  refers to the  $n$ th transverse mode of the straight input lead. From (19) we then have

$$j_L = \phi_n^2(y) \quad (20)$$

for the current density within the lead. The corresponding total current  $I$  is thus equal to 1. If we now take into account reflection  $R$  and transmission  $T$  because of the billiard, we have

$$I = 1 - R = T, \quad (21)$$

which is also the current in the output lead. Furthermore, for any cross section within the cavity itself we have

$$I = \int_{f_1(x)}^{f_2(x)} j_x dy. \quad (22)$$

Finally, an integration of  $I$  over  $x$  from input to output leads gives

$$\langle j_x \rangle = \frac{IL_x}{A} = \frac{TL_x}{A}, \quad (23)$$

in accordance with the definition in (7). For the special case of a rectangular billiard with  $A = L_x L_y$  we have the simple relation

$$\langle j_x \rangle = \frac{I}{L_y} = \frac{T}{L_y}, \quad (24)$$

where  $L_y$  is the height. This relation should be a good approximation, for example, for Sinai and Bunimovich billiards with moderately large circular sections in the reflecting walls.

The elementary expressions above suggest a simple way of estimating  $\langle j_x \rangle$  once  $I$  is known from, for example, measurements. They also explain why the simple isotropic expression in (15) many times turns out to be a good approximation also for cases when  $I$  (or  $T$ ) is large, as found in Ref. [10]. The mean value  $\langle j_x \rangle$  simply takes a small value when  $L_y$  happens to be large.

### IV. NUMERICAL RESULTS FOR AN OPEN CHAOTIC SINAI BILLIARD

As a numerical application and verification of the analytic expressions above for  $P(j_x)$  we consider an open two-dimensional Sinai hard-walled billiard coupled to a pair of opposite leads of width  $d$ , as in the inset in Fig. 2. In [10] numerical results for the current statistics for the Bunimovich stadium was compared with theory, assuming that the net current density could be approximately set equal to zero as in (15). One reason for the small current density was the particular choice of perpendicular leads. In the present case opposite leads are lined up perfectly in order to facilitate directional flow and a noticeable net current, as will be seen below.

The size of the rectangular part in Fig. 2 is  $L_x \times L_y$ , and  $R$  the radius of the circular cutoff. Here we let  $L_y/L_x = 4/3$  and  $R = L_x/6$ . In the computations, we have made use of the finite difference method with a  $600 \times 800$  numerical grid for the rectangular area. Two different cases of small and large aspect ratios, namely  $d/L_y = 1/20$  and  $d/L_y = 1/10$ , have been selected. In the numerical computations we have used  $d$  as a characteristic length scale. The dimensionless wave frequency is therefore  $\omega = dk$ , where  $k$  is the wave number.

Figure 2 shows the transmission probability vs frequency  $\omega$  of the incident wave for single-channel transmission. Case (A) corresponds to minimal transmission  $T \approx 0$  and  $\langle j_x \rangle \approx 0$  and (D) corresponds to  $T = 0.5$  for which  $\langle j_x \rangle \neq 0$ . For both (B) and (C) the transmission is maximal or nearly so. For cases (A) and (B) the aspect ratio is small, while it is chosen large for (C) and (D). Before presenting the numerical results it is useful to rewrite the definition of averages in (7) as

$$\langle F \rangle = \frac{1}{N} \sum_j F_j, \quad (25)$$

where  $N$  is the number of points of a two-dimensional computational grid in the interior of the billiard. The wave function inside the billiard is normalized as

$$\frac{A}{N} \sum_j |\psi_j|^2 = 1. \quad (26)$$

Relevant mean values are collected in Table I. The averages  $\langle p \rangle$ ,  $\langle p_x \rangle$ ,  $\langle q \rangle$ , and  $\langle q_x \rangle$  are not listed in Table I since they are

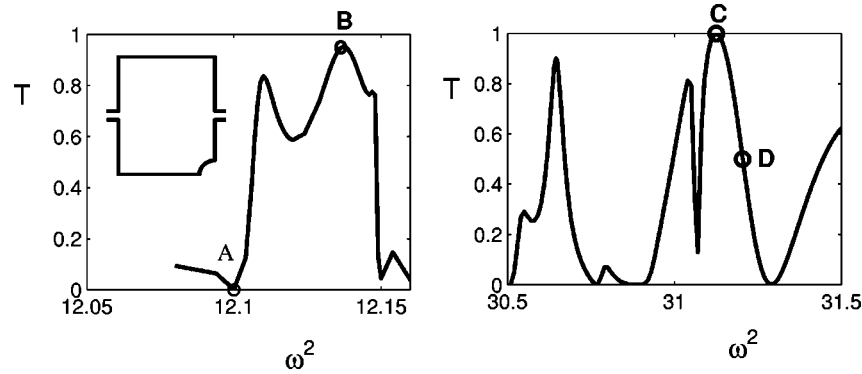


FIG. 2. The transmission probability  $T$  as a function of  $\omega^2$  for single-channel transmission with  $\omega = kd$ . (For electron quantum transmission  $\omega^2$  should be replaced by  $E/E_0$ , where  $E_0 = \hbar^2/2md^2$  and  $m$  is the electron mass). The inset shows the hard-walled Sinai billiard with two opposite aligned leads. The cases of small and large aspect ratios  $d/L_y = 1/20$  and  $d/L_y = 1/10$  are shown in the left and right panels, respectively. The statistics discussed in the text refer to (A)–(D).

negligibly small;  $\langle j_y \rangle$  is also omitted since it must vanish for the present case.

From Table I we find that the random field inside the billiard is effectively isotropic, i.e.,  $D_1 \approx D_2$ , when  $T$  is close to zero (case A). Figure 3 shows the statistics for the wave function and currents for this case. As shown in the inset the real part of  $\psi$  obviously obeys a Gaussian distribution

$$f(p) = \int dq_x f(p, q_x) \quad (27)$$

very closely, as it should for a random field. The parameter

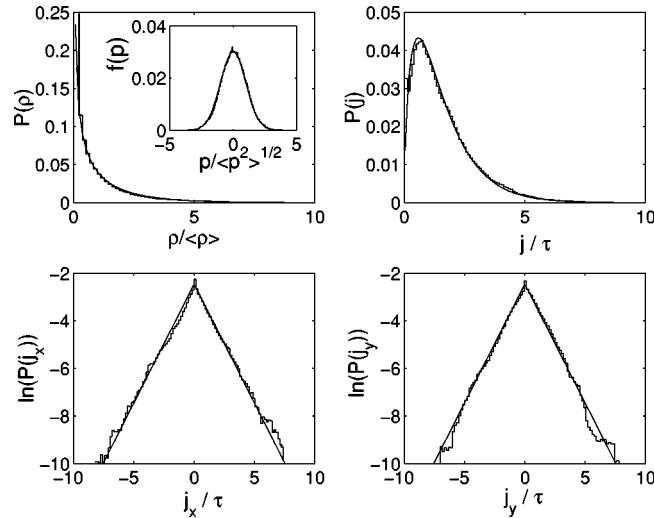


FIG. 3. Statistics for the transmission through the Sinai billiard for  $T \approx 0$  (case A shown in Fig. 2). The upper left panel shows the computed distribution for  $\rho = |\psi|^2$  together with the Porter-Thomas distribution  $P(\rho)$  (solid curve). In the inset of the same panel the computed wave-function statistics  $f(p)$  for the real part of  $\psi$  is compared with a random Gaussian distribution (solid curve). In the upper right panel the distribution for the current density  $P(j)$  is shown together with the theoretical prediction for the case  $\langle j_x \rangle = 0$ . Lower panels show the computed distributions for the  $x$  and  $y$  components of  $\mathbf{j}$  on a logarithmic scale together with the analytic expression (15) (straight solid lines).

$$\epsilon = \sqrt{\frac{\langle q^2 \rangle}{\langle p^2 \rangle}} \quad (28)$$

in Table I gives the relative importance of the real and imaginary parts of the scattering wave function in (4). For case A the imaginary part evidently dominates. As a result there is a very small net current density which is consistent with the small transmission probability as in (24). Since  $p \ll q$ , the distribution function of the squared modules  $\rho = |\psi|^2 = p^2 + q^2$  is described well by the Porter-Thomas distribution  $P(\rho) = (1/\sqrt{2\pi\rho}) \exp(-\rho/2)$  for closed billiards with time reversal [2]. Evolution of the distribution  $P(\rho)$  with increasing transmission probability is given in [9].

The parameter  $\epsilon$  in (28) is closely related to the phase rigidity of the wave function, introduced by van Langen *et al.* [23],

$$r = \frac{|\langle p^2 \rangle - \langle q^2 \rangle|^2}{(\langle p^2 \rangle + \langle q^2 \rangle)^2}. \quad (29)$$

The relation between these two parameters is simply

$$r = \left( \frac{1 - \epsilon^2}{1 + \epsilon^2} \right)^2. \quad (30)$$

The parameter  $r$  measures the phase rigidity of a chaotic complex wave function in the transition between a closed billiard and a completely open one. We presented in Table I both parameters  $\epsilon$  and  $r$ . One can see from Table I that these parameters strongly fluctuate with frequency. The distribution  $P(r)$  was first calculated in [24,25], which is important to consider for averages over a frequency window [19]. However, here we consider statistics for single-mode transmission at a given fixed frequency.

Our computed current distributions  $P(j_x)$  and  $P(j)$  for  $j = \sqrt{j_x^2 + j_y^2}$  are also displayed for case A in Fig. 3. The numerical results, which derive from all points in the billiard, are evidently well described by the analytic expression (15) for zero net current density and the related expression for  $j$  derived in [10]. We thus conclude that the wave function is nearly real at small transmission and is well approximated by a real isotropic random field for cases like A. Hence, the

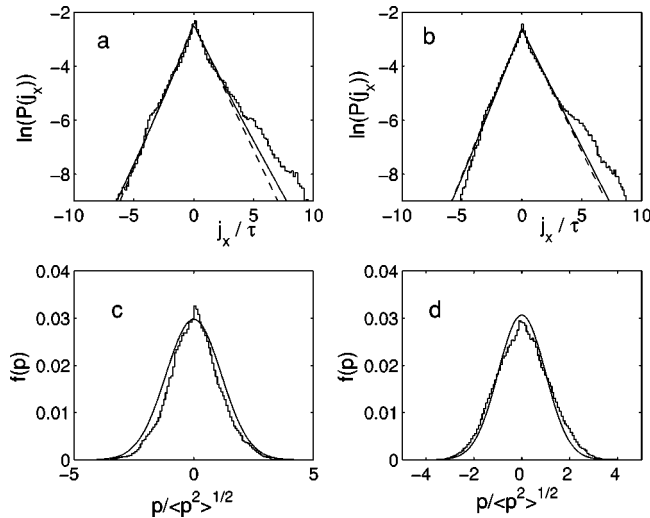


FIG. 4. Current and wave-function statistics for the transmission through the Sinai billiard for the cases D (a, c) and C (b, d) shown in Fig. 2. Thin straight lines in (a, b) refer to the exact formula (18) and dashed lines to the simplified expression in (13). Wave-function statistics are shown for the real part  $p$  of  $\psi$  in (4). The statistics for the imaginary part  $q$  show similar behavior. Thin solid curves in (c, d) refer to the Gaussian distributions in  $f(p)$  in (27).

Thomas-Porter distribution and the isotropic current distribution in (15) apply. In case B the net current density is finite,  $\langle j_x \rangle/k=0.023$ , and the mixture of real and imaginary parts  $p$  and  $q$  is intermediate with  $\epsilon=0.377$ . The current statistic is therefore asymmetric for  $j_x$ , while it remains symmetric for  $j_y$ , as in Fig. 3. The numerical difference between expressions (13) and (18) is small and both of them apply over 4 orders of magnitude. In the right tail, however, there is a characteristic deviation from the universal distribution.

We now turn to the statistics at the larger aspect ratio  $d/L_x=1/10$ . Thus, cases D and C show larger net current densities  $\langle j_x \rangle$  than case B, in spite of its large transmission. The corresponding current and wave-function statistics are shown in Fig. 4. As for case B the difference between the two analytic forms for  $P(j_x)$  is small and there is good agreement between theory and numerical simulations over several orders of magnitude. The structure in the right tail is very much the same as found for case B.

It is surprising that the difference between the exact formula and the approximate one is so small in spite of quite a large anisotropy of the scattering function (Table I). However, for larger currents along transport (for  $j_x/\tau$  roughly exceeding 5) there is, as mentioned, a noticeable difference between analytic formulas and numerical statistics. However, if plotted on a linear scale as in Fig. 5, this difference appears quite small. In Figs. 4(c) and 4(d) we notice also that distributions of the real/imaginary parts of the scattering function  $p$  and  $q$  do not fit perfectly to the Gaussian distributions. We therefore conclude that the more the billiard becomes open because of the leads, the less may the scattering function be described as a random Gaussian complex field.

## V. CONCLUDING REMARKS

We have considered distributions for scattering wave-function amplitudes (real or imaginary parts  $p$  and  $q$ ) and of

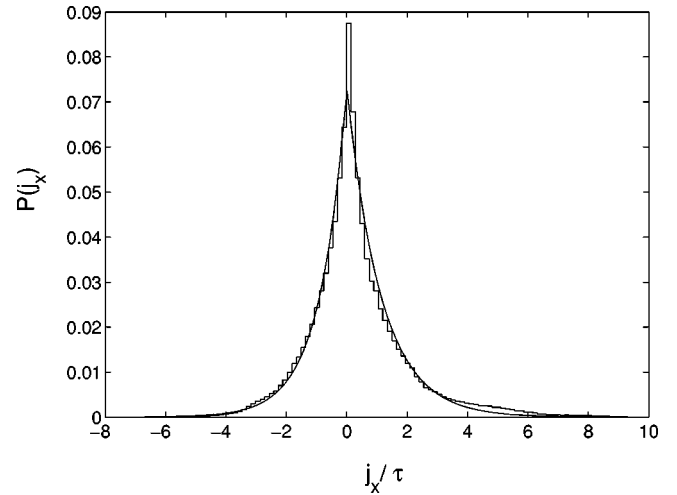


FIG. 5. Current statistics for case D in Fig. 2. The thin solid line shows the exact formula (18).

the components of the current density (Poynting vector) for an open Sinai billiard with two opposite attached straight leads. We have found that the net current  $\langle j_x \rangle$  with  $x$  as the transport axis is proportional to  $T/L_y$ . Assuming that the real and imaginary parts of the scattering function are random Gaussian fields [10] and following Ebeling [21,22], we have derived an analytic distribution for the current components. We have also solved for the true scattering wave function by numerical methods.

The distributions have been studied for different values of the transmission and net currents that increase from zero to finite values. For small net currents the statistics are found to be perfectly described by analytical distribution functions. As the net current is increased, however, the statistics of the scattering function are found to deviate from predictions based on the random Gaussian fields. Even at rather small net current densities, as for C and D in Fig. 2, for which the wave-function statistics are approximately described by the Gaussian distribution as in Figs. 4(c) and 4(d), the current statistics have noticeable features for large currents as shown in Figs. 4(a) and 4(b). To find a plausible reason for the deviation we proceed in the following way. In line with [26] Fig. 6 shows how the current flow for the true scattering state may be decomposed into “internal” and “external” parts. The internal part never makes connection with the leads and therefore does not contribute to the net transport through the

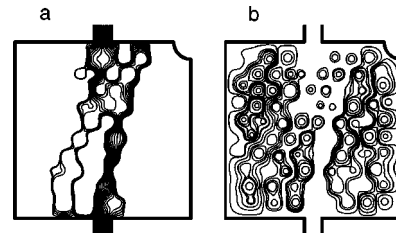


FIG. 6. Flow lines in a rectangular Sinai billiard with numerical sizes. (a) Only flows connecting input and output leads are shown. (b) Internal flows which do not contribute to the net current are shown.

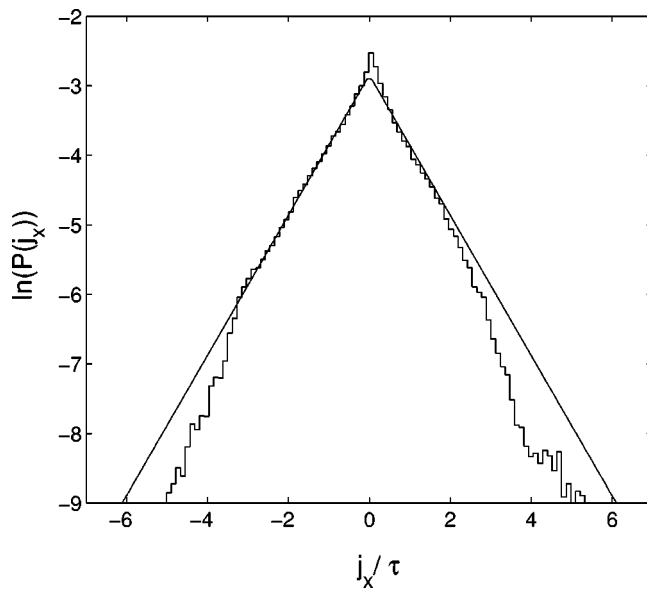


FIG. 7. Statistics of “internal” currents on a logarithmic scale for case C shown in Fig. 4. The area over which the statistics were computed does not intersect the external flow lines shown in Fig. 6. The solid line shows the analytical distribution (15) for which  $\langle j_x \rangle = 0$ .

cavity. Consequently, the net current is carried by the external part. It is noteworthy that the “internal” currents occupy a major fraction of the billiard and that vortices are related to these currents only.

To demonstrate that small tails in the current distributions shown in Fig. 2 are related to the “external” currents we have performed statistics over the area in which only “internal”

currents circulate. The results displayed in Fig. 7 show that the internal currents are isotropic and follow the simple analytic form for  $P(j_x)$  in (15) over several orders of magnitude. Deviations in the tails are opposite the full statistics, including both “internal” and “external” currents. Therefore the detailed behavior of the tails in Fig. 2 are related to the net current flow between the two opposite leads.

In conclusion, we have shown that the current statistics for an open chaotic electron/microwave billiard may, to a good approximation, be obtained by simply replacing the true scattering wave function by a complex Gaussian random field. The agreement with numerical simulations is indeed satisfactory over several orders of magnitude. In spite of the neglect of boundary effects the simple random-field model thus proves quite useful. Here we have focused on only two specific applications, but the analysis is relevant also to other classical wave cavities as, for example, open planar acoustic reverberation rooms, elastic membranes, and water surface waves in irregularly shaped vessels.

Finally, we emphasize that the current statistics over the billiard area were considered for a fixed frequency, single-mode, microwave transmission. However, to perform additional averages over the frequency window ensemble, the phase rigidity (30) distribution becomes important [19]. Unfortunately, after such an ensemble average, the current distribution cannot be derived in simple analytic forms as in (13).

#### ACKNOWLEDGMENTS

We are grateful to Anton Starikov for an assistance in numerical computation. This work was supported by the Royal Swedish Academy of Sciences and the Russian Foundation for Basic Research (RFBR Grant No. 04-02-16408).

- 
- [1] S. W. McDonald and A. N. Kaufman, Phys. Rev. Lett. **42**, 1189 (1979); Phys. Rev. A **37**, 3067 (1988).  
 [2] C. Porter and R. Thomas, Phys. Rev. **104**, 483 (1950).  
 [3] H.-J. Stöckmann, *Quantum Chaos: An Introduction* (Cambridge University Press, Cambridge, 1999).  
 [4] A. Kudrolli, V. Kidambi, and S. Sridhar, Phys. Rev. Lett. **75**, 822 (1995).  
 [5] C. Ellegaard, K. Schaadt, and B. Bertelsen, Phys. Scr., T **T90**, 223 (2001).  
 [6] K. Schaadt, G. Simon, and C. Ellegaard, Phys. Scr., T **T90**, 231 (2001).  
 [7] E. J. Heller, Phys. Rev. Lett. **53**, 1515 (1984).  
 [8] A. I. Saichev, K.-F. Berggren, and A. F. Sadreev, Phys. Rev. E **64**, 036222 (2001).  
 [9] H. Ishio, A. I. Saichev, A. F. Sadreev, and K.-F. Berggren, Phys. Rev. E **64**, 056208 (2001).  
 [10] A. I. Saichev, H. Ishio, A. F. Sadreev, and K.-F. Berggren, J. Phys. A **35**, L87 (2002).  
 [11] K. Zyczkowski and G. Lenz, Z. Phys. B: Condens. Matter **82**, 299 (1991).  
 [12] E. Kanzieper and V. Freilikher, Phys. Rev. B **54**, 8737 (1996).  
 [13] R. Pnini and B. Shapiro, Phys. Rev. E **54**, R1032 (1996).  
 [14] P. Šeba, F. Haake, M. Kus, M. Barth, U. Kuhl, and H.-J. Stöckmann, Phys. Rev. E **56**, 2680 (1997).  
 [15] M. Barth and H.-J. Stöckmann, Phys. Rev. E **65**, 066208 (2002).  
 [16] Y.-H. Kim, M. Barth, and H.-J. Stöckmann, Phys. Rev. B **65**, 165317 (2002).  
 [17] Y.-H. Kim, M. Barth, U. Kuhl, and H.-J. Stöckmann, Prog. Theor. Phys. Suppl. **150**, 105 (2003).  
 [18] F. J. Fahy, *Sound Intensity*, 2nd ed. (E&FN Spon, London, 1995).  
 [19] P. W. Brouwer, Phys. Rev. E **E68**, 046205 (2003).  
 [20] M. V. Berry and M. R. Dennis, Proc. R. Soc. London, Ser. A **456**, 2059 (2000) and references therein.  
 [21] K. J. Ebeling, Opt. Acta **26**, 1505 (1979).  
 [22] K. J. Ebeling, *Statistical Properties of Random Wave Fields in Physical Acoustics: Principles and Methods* (Academic, New York, 1984).  
 [23] S. A. van Langen, P. W. Brouwer, and C. W. J. Beenakker, Phys. Rev. E **55**, R1 (1997).  
 [24] H.-J. Sommers and S. Iida, Phys. Rev. E **49**, R2513 (1994).  
 [25] V. I. Fal’ko and K. B. Efetov, Phys. Rev. B **B50**, 11267 (1994).  
 [26] K.-F. Berggren, A. F. Sadreev, and A. A. Starikov, Phys. Rev. E **66**, 016218 (2002).